

## Effects of openings geometry and relative area on seismic performance of steel shear walls

Ali Massumi<sup>\*</sup>, Nasibeh Karimi<sup>a</sup> and Mostafa Ahmadi<sup>b</sup>

Department of Civil Engineering, Faculty of Engineering, Kharazmi University, Tehran, 15719-14911, Iran

(Received February 8, 2018, Revised June 22, 2018, Accepted June 25, 2018)

**Abstract.** Steel shear wall possesses priority over many of the current lateral load-bearing systems due to reasons like higher elastic stiffness, desirable ductility and energy absorption, convenience in construction and implementation technology, and economic criteria. Besides these advantages, this system causes increase in the dimensions of other structural elements due to its high stiffness as one of its intrinsic characteristics. One of the methods for stiffness reduction is perforating the wall panel and creating openings in the wall that can also be used as windows or ducts in buildings service period. The aim of the present study is probing the appropriate geometric shape and location of opening to fulfil economic criterion plus technical and seismic design criteria. In the present research, a number of possible while reasonable opening shapes and locations are defined in various sizes for some steel shear wall specimens. The specimens are modelled in ABAQUS finite elements software and analyzed using nonlinear pushover analysis. Finally, the analyses' results are reported as force-displacement diagrams and the strength, the initial stiffness and the energy absorption are calculated for all specimens and compared together. The obtained results show that both shape and location of the openings affect the seismic parameters of the shear wall. The specimens in which the openings are further from the center and closer to the columns possess higher stiffness and strength while the specimens in which the openings are closer to the center show more considerable changes in their seismic parameters in response to increase in opening area.

**Keywords:** steel shear wall; openings' geometric shape; openings' location; seismic performance; nonlinear pushover analysis

### 1. Introduction

In recent years, there has been a considerable progress in earthquake resistant design of buildings, and the designs that are based on providing sufficient stiffness and strength have been replaced by modern design systems in which energy absorption and dissipation has a significant role. Modern methods have considerably reduced materials consumption through utilizing appropriate energy dissipaters in structures that besides providing economic justification, they ameliorate structural behavior and its technical criteria. Moreover, parallel to progression of systems, analysis and design methods have significantly progressed. These methods model the materials and elements' behavior with a high precision and apply the seismic effects to structures in a more realistic manner.

To resist lateral forces, specifically seismic forces, various systems are used and dual systems comprised of moment resisting frames along with some other supplemental system are among them. Thin steel shear walls have been recently used as a supplement to moment frames in dual systems and have gained wide acceptance

due to quick implementation and economic justification. One of the drawbacks of steel shear walls is that they are usually implemented with a higher thickness than the design demand due to practical limitations. This leads to enhancement of the dimensions of beams, columns and their connections that result in demand increase of the buildings foundation so these elements are designed for internal plane resistance of the shear wall. To overcome this disadvantage, the stiffness of wall should be lessened to the demand level. One of the proposed options to achieve this aim is using light grade, cold-formed, low-yield-strength steel for internal plane of the wall. Another possible solution for decreasing the applied force to the boundary elements is drilling holes in the plane to reduce the plane's strength and stiffness besides utilizing reduced beam sections (RBSs) at the ends of horizontal boundary elements. In addition to reducing the stiffness and demands of other structural elements, these openings can enhance the serviceability of the walls when they are used as windows, doors or ducts. Thorburn *et al.* (1983) conducted a comprehensive study on steel shear walls. They showed that infill plate buckling under lateral load does not represent the ultimate capacity of steel shear walls and diagonal tension field dominates post-buckling behavior. Elgaaly *et al.* (1993) utilized a finite element model to investigate the results of experimental models that were studied by other researchers. They showed that the strength of the wall does not significantly increase when the plate is thicker because

\*Corresponding author, Professor,  
E-mail: [massumi@khu.ac.ir](mailto:massumi@khu.ac.ir)

<sup>a</sup> M.S., E-mail: [n.karimi2@yahoo.com](mailto:n.karimi2@yahoo.com)

<sup>b</sup> M.S., E-mail: [mahmadi.g.s@gmail.com](mailto:mahmadi.g.s@gmail.com)

yielding of the column had been the dominant factor in both considered thicknesses. Xue and Lu (1994) conducted an analytic study on four 12-story, 3-span shear walls. It was found that beam to column connection type does not have considerable effects on force-displacement behavior of the system and connecting the panels to the columns causes a relatively low increase in the ultimate capacity of the system. They concluded that by connecting the plates only to the beams and using simple beam to column connections, an optimum case is achieved because this condition diminishes shear forces in columns and precludes column sudden rupture. In another research, a numerical model named modified frame-plate interaction model was proposed for shear and bending analysis of ductile steel shear walls (Kharrazi *et al.* 2004). In this study, the data of Driver's experiment (Driver *et al.* 1998a) was employed to evaluate the modified frame-plate interaction model. The model estimates the initial stiffness 5% higher and the ultimate capacity some 10% lower; it also estimates sample's capacity in the yielding's onset slightly higher. Based on the analytic method of Thorburn *et al.* (1983), Timler and Kulak (1983) tested two full-scale one-story one-span samples with infill panels. Researchers have conducted other experimental tests on steel shear walls (Tromposch and Kulak 1987, Lubell 1997, Driver *et al.* 1997, 1998a, Schumacher *et al.* 1997). Astaneh-Asl (2001) considered a steel shear wall sample for his experiment that in fact was a model of internal core of The Seattle's Courthouse. He also did a pushover finite element analysis on his experimental models and concluded that the finite element model was only capable of describing the general behavior and ultimate capacity of the steel shear wall.

To reduce applied force to boundary elements, Vian and Bruneau (2004) did tests on samples that included perforated steel panels and steel panels with cut corners. All samples had beam to column connections with Reduced Beam Sections (RBS) details at the ends only to decrease top and bottom beam dimensions and to prevent formation of plastic hinge in the middle of the beam. The obtained hysteretic curves of the perforated panel sample indicated a steady behavior in spite of strength and stiffness reduction compared with imperforated sample. They also presented equations to approximate stiffness reduction of the panel due to presence of the holes. Valizade *et al.* (2012) experimentally studied the effects of opening dimensions as well as slenderness factors of plates on the seismic behavior of steel plate shear walls. The obtained ductility of specimens showed the stable functioning of the system in the nonlinear range. They concluded that although the stable cyclic behavior of specimens in the nonlinear range causes mostly a dissipation of energy during the loading of samples, but existence of an opening at the center of the panel causes a noticeable decrease in energy absorption of the system. Darilmaz (2017) carried out a vibration study on orthotropic elliptic paraboloid shells with openings using a hybrid stress finite element. In his study, natural frequencies of orthotropic elliptic paraboloid shells with and without openings were presented. He also investigated the influence of aspect ratio, height ratio, opening ratio and material angle on the frequencies and mode shapes.

In the presents study, the effect of geometric shape of opening on seismic performance of the wall is investigated. By selecting various reasonable shapes for shear wall openings, their seismic characteristics are determined and compared so that it is cleared to what extent the shear wall opening shape affects its performance and which shape can offset the steel shear wall drawbacks more effectively. To this end, the S2 experimental specimen of Vian and Bruneau (2004) is initially modeled using ABAQUS software and the models are verified by comparing analytic and experimental results. Then various openings with different shapes and dimensions are defined in the same shear wall and nonlinearly analyzed after they are modeled in the software. Finally, by summing up the acquired data of the models, the responses are compared in the form of stiffness, ductility and strength parameters.

## 2. Description and verification of the utilized models

To model the samples having openings, the steel shear wall of Vian and Bruneau (2004) is considered in which the openings with various shapes and dimensions are contrived. The steel shear walls with openings are divided into two groups. In the first group, the area of openings is less than half of the area of the wall panels (the openings area is set to be 10%, 20%, 30%, 40% and 50% of the panel area in different cases) and the area of the openings is more than half of the area of the wall panels in the second group (the openings area is set to be 70%, 80%, and 90% of the panel area in different cases).

Considering the openings' dimensions, a few different shapes are assigned in each case. For the first group, six varied shapes are defined for openings so that forms 1 to 4 may have 10%, 20%, 30%, 40% and 50% openings area whereas forms 5 and 6 may possess 10%, 30% and 50% openings area. In the second group, four varied openings shapes are defined so that forms 1 and 3 may have 70%, 80% and 90% openings area whereas forms 2 and 4 may have 70% and 80% openings area. The reason for assigning 70%, 80% and 90% openings areas to the shear walls has been to consider feasible openings cases where the steel

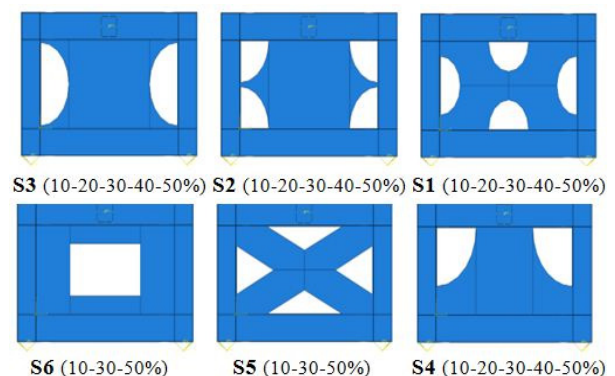


Fig. 1 Schematic representation of the six considered shapes with 10 to 50 percent openings area

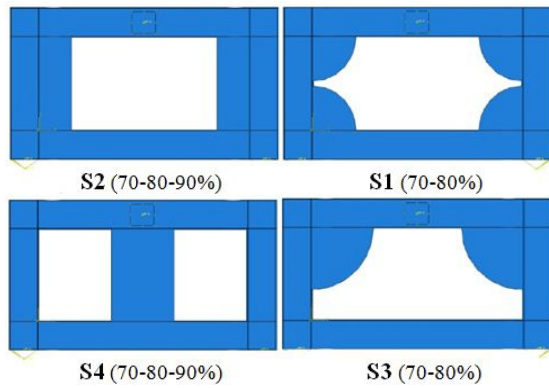


Fig. 2 Schematic representation of the four considered shapes with 70 to 90 percent openings area

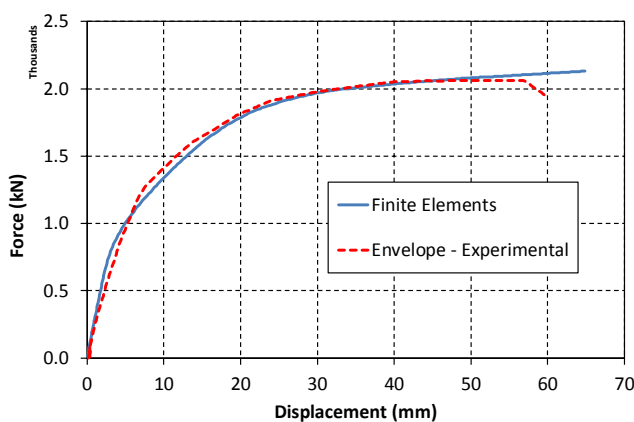


Fig. 3 Comparison of hysteresis loops envelope of Vian's experimental test and the force-displacement diagram of analytic model

shear wall acts merely as stiffener in the frame. In Figs. 1 and 2 the schematic representations of considered opening shapes for the first and the second groups are depicted respectively. In all cases, the opening shapes are symmetrical relative to one or both perpendicular axes that pass through the center of the wall panels.

Fig. 3 represents the force-displacement diagram of the analytic model of Vian's specimen in ABAQUS along with hysteresis loops envelope of the experimental test's results. It is observed that the initial stiffness of the finite elements model is slightly higher than that of the experimental model and there is a negligible difference in the two model's ultimate force. These differences could be explained by the imperfections that exist in experimental settings and as the type, amount and place of these imperfections are indefinite, they could not be precisely applied in finite

element modelling.

Moreover, the existence of residual stresses in experimental model could be among the most effective causes of difference between experimental and finite element models in the nonlinear region. It should be mentioned that in the experimental model, instability of loading regime when applying the pre-determined displacement to the specimen has resulted in generation of torsion in the center of the top beam.

Considering the achieved precision and agreement of analytic and experimental results, we can accept the utilized finite elements model as a reliable model to predict the behavior of steel shear wall specimens.

### 3. Results of analyses

Numerical models of all example cases which included frame and infill steel panel are analyzed using ABAQUS finite elements modelling program. In the present study, Static General Method is used that is among most typical analysis methods in ABAQUS. Abrupt out-of-plane deflection of the steel panel leads to convergence problems in analysis of steel panel shear walls due to the extension of tension field. While it is possible to model boundary elements with Beam element, but if local buckling occurs in them it will not be considered in the analysis. To include lateral buckling, the boundary elements and panels are modeled with Shell, S4R element that is a four-node two-curve element with reduced integrating. Each node has six degrees of freedom (DOFs): three translational and three rotational DOFs. All the utilized materials in the models are isotropic with inelastic bilinear stiffening behavior. Tension and compression behaviors are defined in the same way. Characteristics of applied materials in wall elements are defined according to Table 1. Other assumptions are according to previously mentioned Vian's model premises. Mesh sizes are set to 75 and 50 mms for examples with less than 50% and more than 50% openings area respectively. In some cases, however, for program's analytic problems solving, mesh sizes are slightly smaller or bigger wherever needed.

As the results of uniform loading fashion well agree with the results of pseudo-static (pseudo-dynamic) loading, the loading on samples is exercised uniformly. Cyclic pseudo-static loading that is in fact a kind of seismic loading simulation, follows the rules of ATC-24 Code (1992).

Fig. 4 represents the applied loading history to Vian's experimental specimens. To apply the loading uniformly, the envelope of pseudo-static loading is obtained and the loading is applied to the models accordingly. Vian's

Table 1 Materials characteristics of steel shear wall specimens

Element	Yield stress (MPa)	Ultimate stress (MPa)	Ultimate strain	Modulus of elasticity (MPa)	Poisson's ratio
Frames (beams and columns)	345	500	0.15	200000	0.3
Wall panel	165	300	0.15	200000	0.3

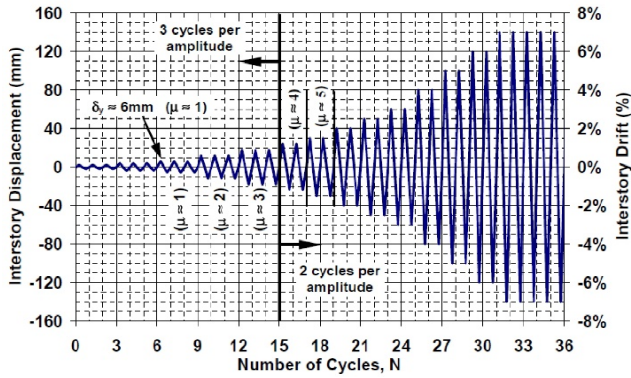


Fig. 4 Applied loading history to Vian's experimental specimens (2004) in pseudo-static loading

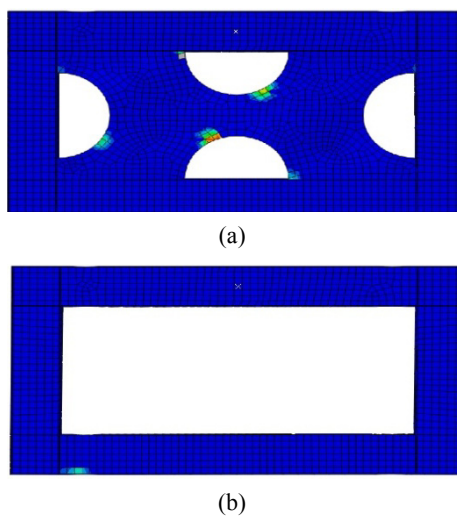


Fig. 5 Yielding onset location in S1-30% specimen: (a) infill panel; (b) wall frame

experimental specimens are loaded up to 3% and 4% relative displacement in imperforated and perforated specimens respectively. In the present research, as the program is not able to model local fractures arose during loading that brings about strength drop, the loading is continued up to 4.5% relative displacement.

### 3.1 Sample of analysis results of the first group

Fig. 5 indicates the yielding onset location in the wall infill panel and the frame of S1-30% specimen. According to Fig. 5(a), yielding in the panel starts from corners and edges of the longitudinal openings and as the loading increases (increase in displacement), corners and edges of the transverse openings yield too. In the wall frame, yielding commences from Reduced Beam Section (RBS) of the bottom beam in the side under tension (Fig. 5(b)) and extends to the RBS in the top at the other end of the wall's diagonal. At the loading peak, beam to column connections yield too (Fig. 6). Fig. 6(a) demonstrates Mises stress in the wall panel at the yielding onset. At this time, the stress in illustrated locations reaches 166.3 MPa that corresponds to 2.47 mm displacement. In 16.28 mm displacement, the

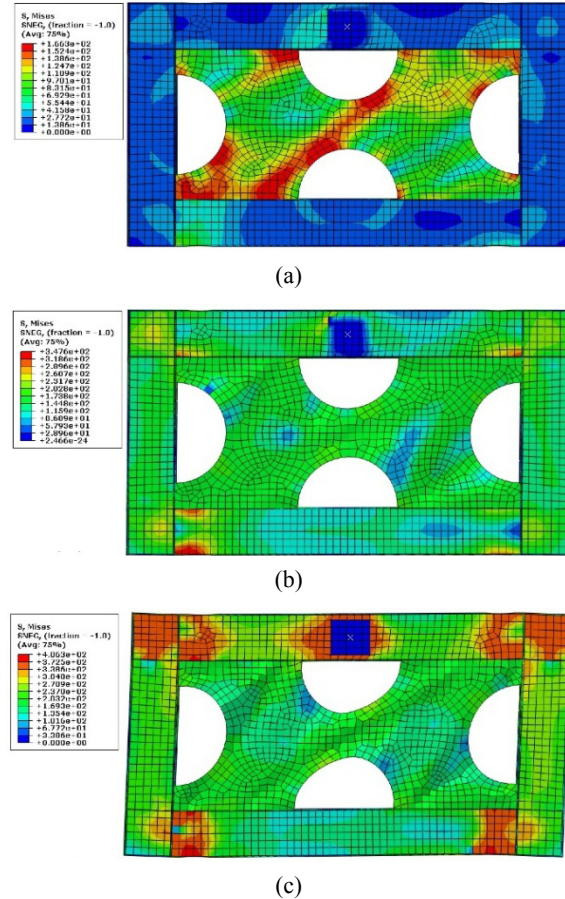


Fig. 6 Stress contours in S1-30% specimen: (a) stress contour at the beginning of yielding in the shear wall panel; (b) stress contour at the beginning of yielding in the shear wall frame; (c) stress contour at the end of loading (4.5% drift) in the shear wall

stress in some parts of the frame reaches the value of 347.6 MPa (Fig. 6(b)). Then the loading continues to 90 mm displacement (4.5% drift). At the end of the loading, the maximum stress in the wall panel reaches 260.7 MPa and reaches 406.3 MPa in the frame.

At this time, according to the results shown in Fig. 6(c), the displacement of the whole shear wall is reported to be 92.69 mm. From Fig. 6 it is clear that the stress in the wall panel under buckling reaches yielding stress threshold and regarding one-way fashion of the loading, diagonal tension field emerges in the wall panel and the load bearing continues; the wrinkles caused by this process are clearly visible in the figure that become deeper as the loading increases.

### 3.2 Sample of analysis results of the second group

Fig. 7 represents the yielding onset location in the wall infill panel and in the wall frame of S2-70% specimen. As can be seen from Fig. 7(a), yielding in the panel starts from inner corners of the two parts of the infill panel where they are connected to the longitudinal beams. The onset of yielding in the frame is from Reduced Beam Section in the two sides of the bottom beam's bottom flange and extends

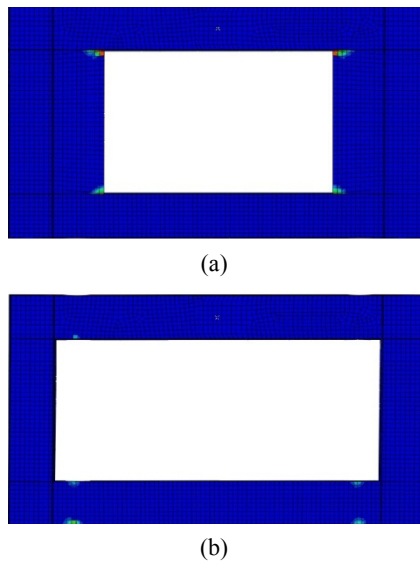


Fig. 7 Yielding onset location in S2-70% specimen:  
(a) infill panel; (b) wall frame

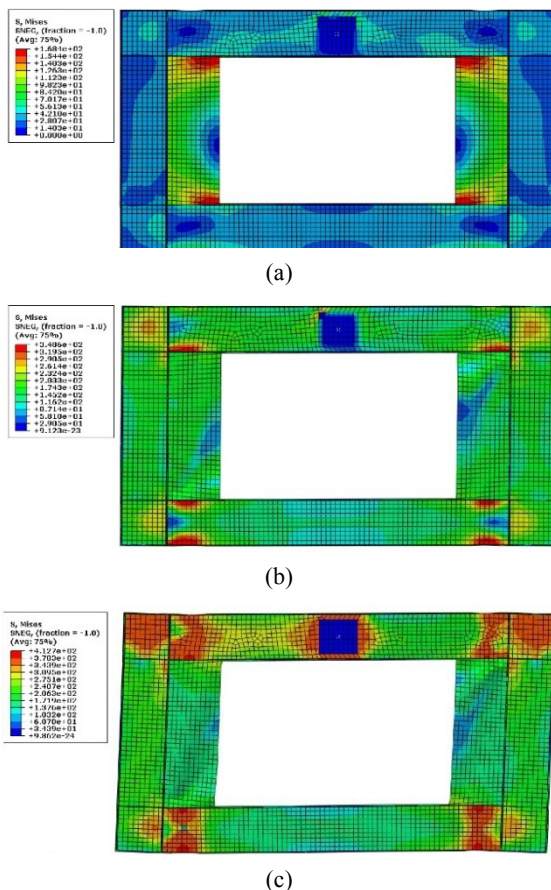


Fig. 8 Stress contour in S2-70% specimen: a) stress contour at the beginning of yielding in the shear wall panel, b) stress contour at the beginning of yielding in the shear wall frame, c) stress contour at the end of loading (4.5% drift) in the shear wall

to the RBS of the top beam (Fig. 7(b)); at the end of the loading beam to column connections yield too (Fig. 8).

Fig. 8(a) shows Mises stress in the wall panel at the yielding onset. At this moment, stress in the indicated locations reaches 168.4 MPa that corresponds to 3.41 mm displacement. In 18.53 mm displacement, the stress in some parts of the frame reaches 348.6 MPa (Fig. 8(b)). At the end of the loading that corresponds to 4.5% relative displacement (90 mm), the maximum stresses are 288.2 MPa in the wall panel and 412.7 MPa in the wall frame. At this instant, the displacement of the whole shear wall is reported to be 93.52 mm. As it can be observed from Fig. 8, while the major part of the wall is empty but the stress in the wall panel under buckling reaches the yielding limit from the very beginning of loading. Considering the one-way fashion of loading, diagonal tension field is formed in each of these existing parts in the wall frame and load bearing continues. The wrinkles resulting from this process can be easily observed in the figure, which become deeper with increase in loading.

#### 4. Comparison of analyses' results

In this section, the analyses' results of the specimens within each of the two previously defined groups are compared. The first group includes the specimens that have 10-50% openings area while the second group contains the specimens with 70, 80 and 90 percent openings area. The values of applied force and corresponding displacements at the yielding time and at the end of the loading, calculated initial stiffness, the strength at the end of the loading and the absorbed energy are represented in a number of tables for each considered case. It is needed to be mentioned that in the present study the criterion of loading termination is not considered fracture occurrence, but rather reaching the relative displacement of 4.5% according to Vian's experimental sample. This is because the software is not able to model the generated local fractures in the specimens during loading process so it is not feasible to determine the exact point in which the specimens reach their maximum strength and the displacements up to which they have load-bearing capacity (the termination point corresponding to universal fracture not being specific).

Therefore, maximum force and displacement at the end of the loading, which corresponds to 90 mm displacement for all specimens, are used as a comparison criterion. The absorbed energy that equals the area under the force-displacement curve is also calculated for each specimen and are compared together. To achieve universal yielding force and displacement, the bilinear curve is delineated from the force-displacement curve of each specimen. In Fig. 9, the bilinear curve for the imperforated specimen is presented. The bilinear curves for other specimens are drawn accordingly.

##### 4.1 Comparison of the first group of specimen (S10%, S20%, S30%, S40%, S50%)

Force and displacement values at the yielding onset time, i.e., the end of linear behavior of the whole steel shear wall, and at the end of the loading are presented for S10%, S20%, S30%, S40% and S50% specimens in Tables 2, 3, 4,

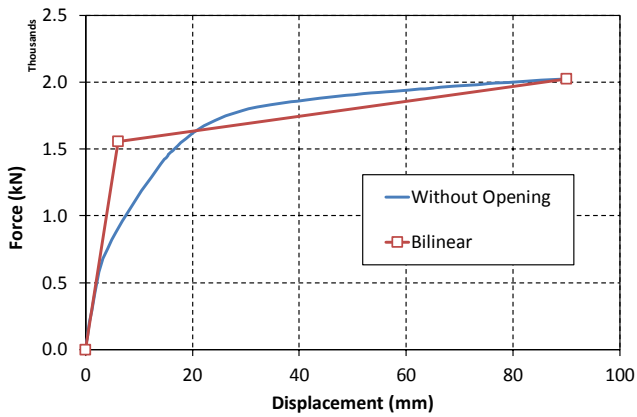


Fig. 9 Force-displacement curve for the imperforated specimen and the corresponding bilinear curve

5 and 6 respectively. In these tables, the initial stiffness, the strength at 90 mm displacement and the absorbed energy are also given for each specimen.

#### 4.1.1 Comparison in terms of stiffness

The diagrams of changes in initial stiffness of specimens with 10%, 20%, 30%, 40% and 50% openings area are presented in Fig. 10 for different openings forms while Fig. 11 represents initial stiffness changes of specimens with S1, S2, S3, S4 and S5 forms for different openings areas. As the

initial stiffness pertains to elastic state of the structure where there has not yet occurred any damage that introduces several parameters relating to inelastic behavior, comparison of the initial stiffness of the considered models (e.g., experimental and finite-elements models) is an appropriate criterion for control and verification of modelling. Moreover, the initial stiffness, due to lack of emergence of the phenomena (such as buckling) that are related to the stiffness after the structure becomes inelastic, can be considered a proper criterion in various numerical models for evaluation of impressibility and sensitivity of the structure to the loading process.

From Fig. 10 and as expected, it is clear that initial stiffness of all specimens decreases with increase in openings area. Fig. 11 shows that forms 4, 3 and then 2 have higher stiffness so it can be inferred that the closer the opening to columns, the stiffer the steel shear wall is and the stiffness reduces when openings get closer to the center of the panel. Form 6 in which the opening is at the center possesses the lowest stiffness that can be related to the diagonal tension field of the wall being more interrupted in this form than other forms.

When forms 1 and 5 that have the same openings locations but different openings shapes are compared, it can be said that form 1 in which the openings have curvy shapes (half circles) are stiffer in all opening areas than form 5 in which the opening are triangularly shaped. This can be associated with stress concentration at the sharp corners of

Table 2 Force and displacement values at yielding instant and at the end of loading; stiffness, strength and absorbed energy of S10% specimens

Specimen	Yielding		Loading end (90 mm)		Initial stiffness	Strength at 4.5%	Absorbed energy
	$U1$ (mm)	$F1$ (kN)	$U2$ (mm)	$F2$ (kN)	$K0 = F1/U1$	$F2$ (kN)	Area under the curve
Imperforated wall	5.8	1730	90	2199.79	298.28	2199.79	170475
10% openings	S1	6.1	1556	90	2021.89	255.08	154844
	S2	6.1	1581	90	2055.30	259.18	157373
	S3	6.1	1581	90	2041.15	259.18	156751
	S4	6.1	1596	90	2051.85	261.64	157906
	S5	6.5	1513	90	1943.47	232.77	149223
	S6	7.1	1500	90	1911.58	211.27	146749

Table 3 Force and displacement values at yielding instant and at the end of loading; stiffness, strength and absorbed energy of S20% specimens

Specimen	Yielding		Loading end (90 mm)		Initial stiffness	Strength at 4.5%	Absorbed energy
	$U1$ (mm)	$F1$ (kN)	$U2$ (mm)	$F2$ (kN)	$K0 = F1/U1$	$F2$ (kN)	Area under the curve
Imperforated wall	5.8	1730	90	2199.79	298.28	2199.79	170475
20% openings	7.0	1450	90	1902.40	207.14	144186	154844
	6.6	1449	90	1921.49	219.55	145335	157373
	6.5	1489	90	1937.22	229.08	147863	156751
	6.1	1468	90	1931.72	240.66	147099	157906

Table 4 Force and displacement values at yielding instant and at the end of loading; stiffness, strength and absorbed energy of S30% specimens

Specimen	Yielding		Loading end (90 mm)		Initial stiffness	Strength at 4.5%	Absorbed energy
	$U1$ (mm)	$F1$ (kN)	$U2$ (mm)	$F2$ (kN)	$K0 = F1/U1$	$F2$ (kN)	Area under the curve
Imperforated wall	5.8	1730	90	2199.79	298.28	2199.79	170475
30% openings	S1	7.8	1353	90	1769.45	173.46	133622
	S2	7.5	1316	90	1744.52	175.47	131202
	S3	7.0	1419	90	1846.81	202.71	140484
	S4	6.9	1385	90	1816.10	200.72	137782
	S5	9.1	1352	90	1688.88	148.57	129139
	S6	9.5	1320	90	1601.32	138.95	123877

Table 5 Force and displacement values at yielding instant and at the end of loading; stiffness, strength and absorbed energy of S40% specimens

Specimen	Yielding		Loading end (90 mm)		Initial stiffness	Strength at 4.5%	Absorbed energy
	$U1$ (mm)	$F1$ (kN)	$U2$ (mm)	$F2$ (kN)	$K0 = F1/U1$	$F2$ (kN)	Area under the curve
Imperforated wall	5.8	1730	90	2199.79	298.28	2199.79	170475
40% openings	S1	9.3	1283	90	1671.07	137.96	125179
	S2,3	8.2	1324	90	1728.46	161.46	130269
	S4	7.9	1311	90	1716.94	165.95	129486

Table 6 Force and displacement values at yielding instant and at the end of loading; stiffness, strength and absorbed energy of S50% specimens

Specimen	Yielding		Loading end (90 mm)		Initial stiffness	Strength at 4.5%	Absorbed energy
	$U1$ (mm)	$F1$ (kN)	$U2$ (mm)	$F2$ (kN)	$K0 = F1/U1$	$F2$ (kN)	Area under the curve
Imperforated wall	5.8	1730	90	2199.79	298.28	2199.79	170475
30% openings	S1	11.9	1245	90	1582.83	104.62	117826
	S2,3	9.5	1276	90	1652.42	134.32	123935
	S4	9.7	1256	90	1627.64	129.48	121892
	S5	11.7	1280	90	1566.59	109.40	118921
	S6	12.0	1241	90	1564.82	103.42	116895

form 5. In specimens with 50% openings area, the stiffness of forms 1 and 5 are almost equal, i.e., when the area of the opening exceeds a threshold the opening's shape does no longer affect the stiffness value. In form 1 with increase in openings area up to 50%, the specimen's stiffness is 15% to 25% reduced for each 10% rise of area in each step. In forms 2, 3 and 4, with increase in openings area up to 50%, the stiffness is 10 to 20% diminished in each 10% area rise step. Forms 5 and 6 have shown the most significant reactions in terms of stiffness change to openings area rise.

#### 4.1.2 Comparison in terms of strength

The diagrams of changes in 4.5% relative displacement

strength of specimens with 10%, 20%, 30%, 40% and 50% openings area are presented in Fig. 12 for different openings forms whereas Fig. 13 shows strength changes of specimens with S1, S2, S3, S4 and S5 forms for different opening areas. Here the term strength corresponds to the strength at 4.5% relative displacement.

From Fig. 12 it can be seen that in all the specimens with various openings forms the strength declines with increase in openings area percentage; the most significant strength decline pertains to the change from imperforated case to 10% openings case. It can also be observed that for each openings area, changes of openings shape does not have a considerable effect on strength. In case of 30%

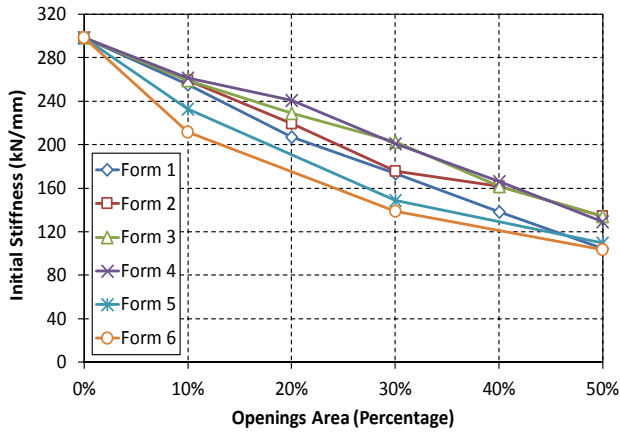


Fig. 10 Changes in initial stiffness of specimens with various openings areas for different openings forms

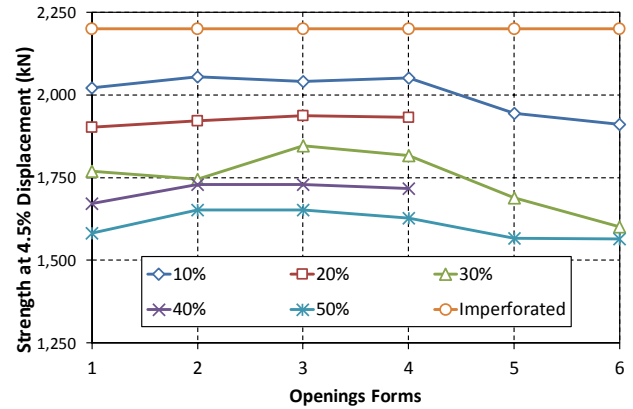


Fig. 13 Changes in strength of specimens with various openings forms for different openings areas

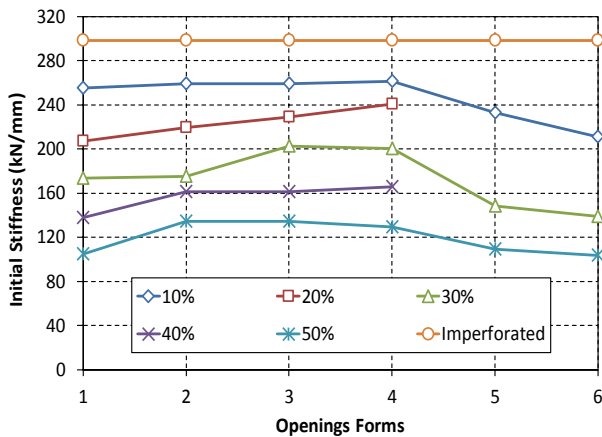


Fig. 11 Changes in initial stiffness of specimens with various openings forms for different openings areas

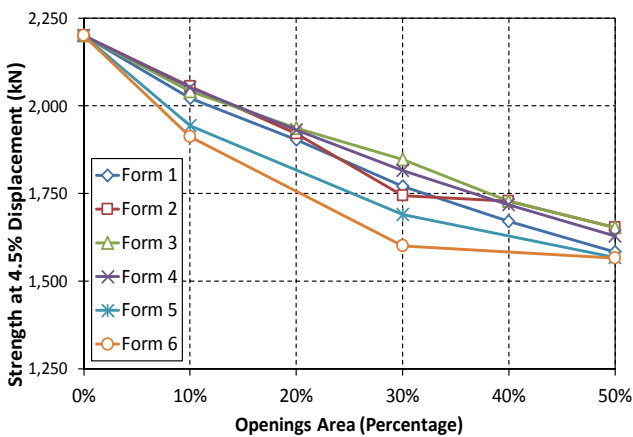


Fig. 12 Changes in strength of specimens with various openings areas for different openings forms

openings the sensitivity to openings form change and its effect on strength is slightly larger. In general, it is seen that for each openings percentage, forms 3 and 4 present the highest strength while the lowest strength values pertain to form 6 and form 5.

It can be observed from Fig. 13, with regard to the effect of shape and location of openings on the strength, that the closer the openings to the columns and the further from the wall's center (forms 2, 3 and 4), the smaller the strength reduction is. Moreover, in similar conditions, the curvier the shapes and without sharp corners, the higher strength the wall represents (comparison of forms 1 and 5). The strength of specimens with forms 5 and 6 reacts to a higher extent than other forms from imperforated case to 10% openings case and from 10% openings case to 30% openings case. The observed declines of strength are five to eight percent in specimens with form 1, four to nine percent in specimens with form 2, four to seven percent in specimens with form 3, and five to six percent in specimens with form 4.

#### 4.1.3 Comparison in terms of energy absorption

The diagrams of changes in energy absorption - which equals to the area under the force displacement curve calculated up to 4.5% relative displacement - of specimens with 10, 20, 30, 40 and 50 percent openings area are shown in Fig. 14 for various openings shapes. Fig. 15 displays the diagram of changes in energy absorption of specimens with different forms for 10 to 50 percent openings area.

Considering the results of Vian's experiment, the specimen cut from the upper two corners suffers fracture

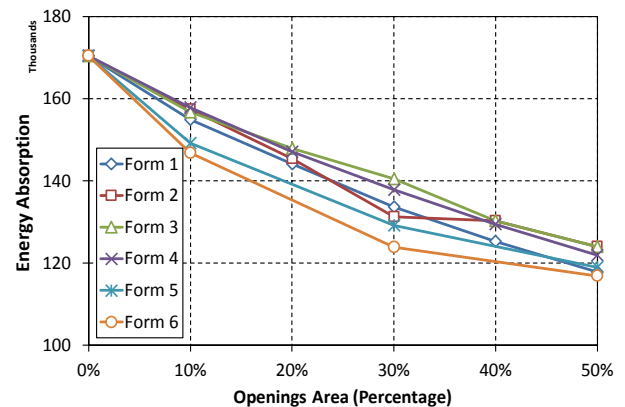


Fig. 14 Changes in energy absorption of specimens with different openings percentages (10% to 50%) for various openings forms

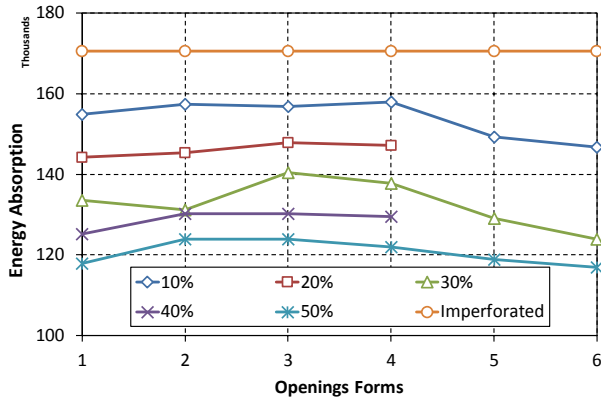


Fig. 15 Changes in energy absorption of specimens with different openings forms (S1 to S6) for various openings percentages

and strength drop after 2.5 to 3 percent relative displacement but bears up to 4% relative displacement. Therefore, in the software models of the present study, the results are valid up to the vicinity of 3 percent drift and become invalidated beyond this displacement because the occurred fractures and failures are not modeled in the software. Accordingly, the energy absorption presented here includes only the elastic behavior region and the region from plastic behavior commencement to occurrence of the first fractures and ruptures in specimens; it does not involve the next region extending from the instance of strength drop to the point of the ultimate fracture. In view of the mentioned conditions, it can be said that the energy absorption (up to 4.5% relative displacement) of specimen with various forms diminishes with increase in openings area percentage from imperforated to 50% openings cases. The trend of this reduction is similar to the trend of decline in stiffness and strength of specimens; in fact, it is the resultant of both strength and stiffness declines and includes both these parameters.

It is seen from Fig. 14 that with increase in openings percentage, the energy absorption trends of specimens with forms 1 to 4 are nearly identical. For each 10 percent rise in openings area in consecutive steps, the specimens with forms 1, 2 and 3 experience between 4 to 9 percent while the specimen with form 4 experience between 5 to 7 percent of energy absorption reduction. The energy absorption

reduction for specimens with forms 5 and 6 have been approximately 13% from imperforated case to 10% openings case, 14% from 10% openings case to 30% openings case and 6.5% from 30% openings case to 50% openings case.

#### 4.2 Comparison of the second group of specimens (S70%, S80%, S90%)

The yielding force and displacement values at the end of linear behavior of the whole steel shear wall and the values of force and displacement at the end of the loading are presented for S70%, S80% and S90% specimens in Tables 7, 8 and 9 respectively. The initial stiffness, the strength at 90 mm displacement and the absorbed energy are also calculated for each specimen and given in these tables.

##### 4.2.1 Comparison in terms of stiffness

The diagrams of changes in initial stiffness of specimens with 70%, 80% and 90% openings area are presented in Fig. 16 for different openings forms while Fig. 17 shows initial stiffness changes of specimens with S1, S2, S3 and S4 forms for different openings areas.

When the initial stiffness of S1 to S4 specimens with 70%, 80% and 90% openings area are compared according to Fig. 16, it is seen that the specimens with forms 1 and 3 and the specimens with forms 2 and 4 possess nearly equal stiffness and the former specimens are stiffer than the latter

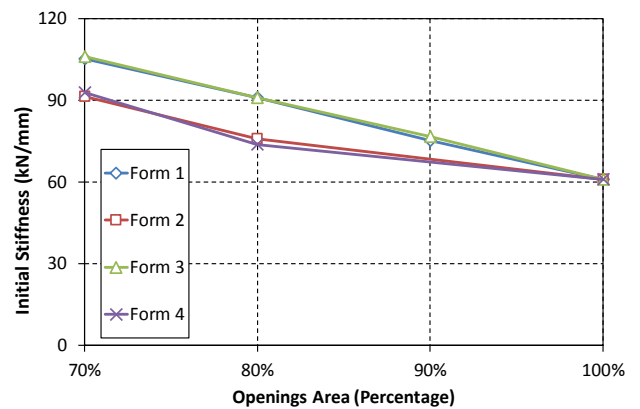


Fig. 16 Changes in initial stiffness of specimens with various openings areas for different openings forms

Table 7 Force and displacement values at yielding instant and at the end of loading; stiffness, strength and absorbed energy of S70% specimens

Specimen	Yielding		Loading end (90 mm)		Initial stiffness $K0 = F1/U1$	Strength at 4.5% $F2$ (kN)	Absorbed energy Area under the curve	
	$U1$ (mm)	$F1$ (kN)	$U2$ (mm)	$F2$ (kN)				
70% openings	S1	11.4	1200	90	1529.32	105.26	1529.32	114112
	S2	13.2	1207	90	1489.08	91.44	1489.08	111483
	S3	11.4	1210	90	1513.27	106.14	1513.27	113915
	S4	13.0	1206	90	1509.87	92.77	1509.87	112388
Just the frame	20.3	1237	90	1420.94	60.94	1420.94	105194	

Table 8 Force and displacement values at yielding instant and at the end of loading: stiffness, strength and absorbed energy of S80% specimens

Specimen	Yielding		Loading end (90 mm)		Initial stiffness	Strength at 4.5%	Absorbed energy	
	$U1$ (mm)	$F1$ (kN)	$U2$ (mm)	$F2$ (kN)	$K0 = F1/U1$	$F2$ (kN)	Area under the curve	
80% openings	S1	13.2	1200	90	1490.26	90.91	1490.26	111222
	S2	15.8	1200	90	1448.80	75.95	1448.80	107768
	S3	13.0	1184	90	1482.17	91.08	1482.17	110360
	S4	16.4	1208	90	1456.54	73.66	1456.54	107973
Just the frame	20.3	1237	90	1420.94	60.94	1420.94	105194	

Table 9 Force and displacement values at yielding instant and at the end of loading: stiffness, strength and absorbed energy of S90% specimens

Specimen	Yielding		Loading end (90 mm)		Initial stiffness	Strength at 4.5%	Absorbed energy	
	$U1$ (mm)	$F1$ (kN)	$U2$ (mm)	$F2$ (kN)	$K0 = F1/U1$	$F2$ (kN)	Area under the curve	
90% openings	S1	16.1	1211	90	1450.34	75.22	1450.34	108070
	S3	15.6	1197	90	1449.73	76.73	1449.73	107796
Just the frame	20.3	1237	90	1420.94	60.94	1420.94	105194	

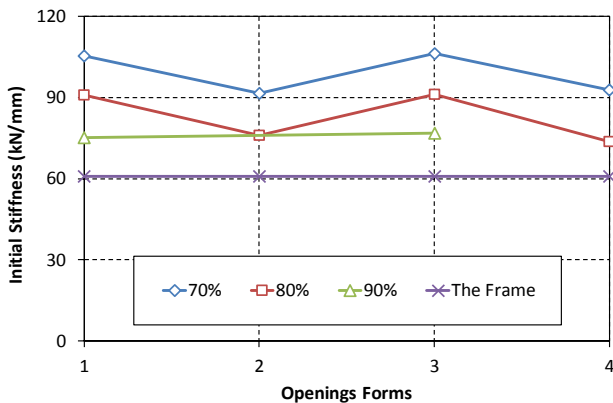


Fig. 17 Changes in initial stiffness of specimens with various openings forms for different openings areas

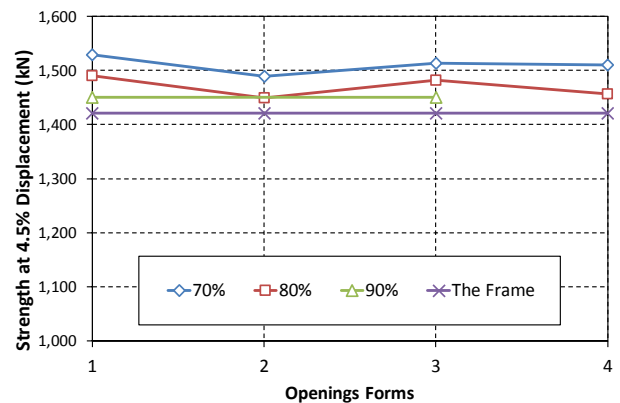


Fig. 19 Changes in strength of specimens with various openings forms for different openings areas

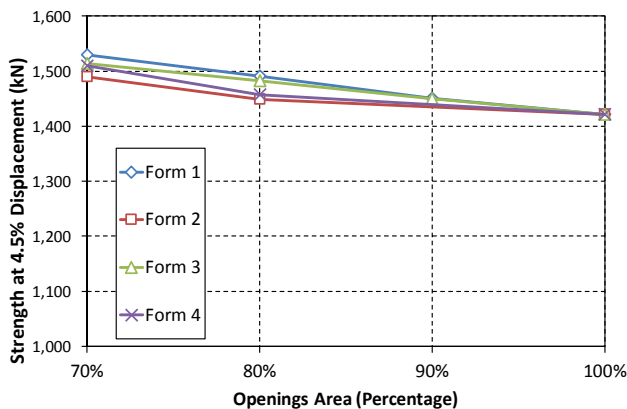


Fig. 18 Changes in strength of specimens with various openings areas for different openings forms

ones. The results of Fig. 17 show that in specimens with forms 1 and 3 the stiffness of the whole shear wall is grown by 20% when 10 percent steel plate is added to the wall frames (comprising the specimens with 90% openings area); while almost the same grow in stiffness of specimens with forms 2 and 4 is achieved by adding 20% steel plate to the frames of these specimens (comprising the specimens with 80% openings area).

#### 4.2.2 Comparison in terms of strength

The diagrams of changes in 4.5% relative displacement strength of specimens with 70%, 80% and 90% openings area are presented in Fig. 18 for different openings forms whereas Fig. 19 displays changes in the strength of specimens with S1, S2, S3 and S4 forms for various openings areas. The strengths of 4.5% relative displacement

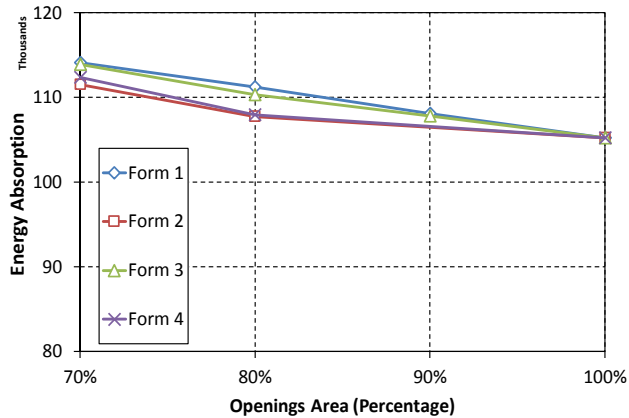


Fig. 20 Changes in energy absorption of specimens with different openings percentages (70% to 90%) for various openings forms

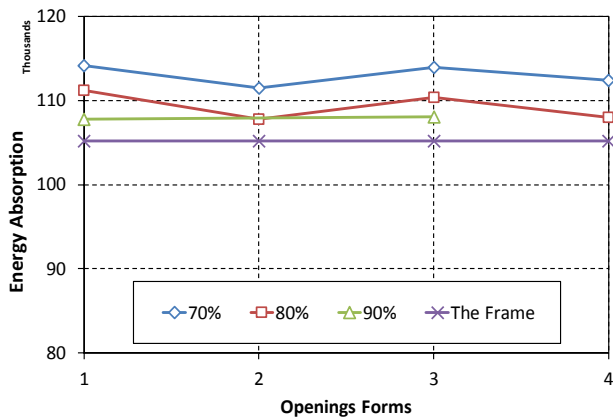


Fig. 21 Changes in energy absorption of specimens with different openings forms (S1 to S4) for various openings percentages

of specimens with 70, 80 and 90 percent openings area do not differ significantly. The decline trend of strength at the end of the loading in all specimens from 70 to 80 and from 80 to 90 percent has a constant gradient. The highest value for this gradient belongs to the specimen with form 4. The change of strength for different forms with various openings area is approximately 2 to 3 percent for each 10 percent increase in openings area.

#### 4.2.3 Comparison in terms of energy absorption

The diagrams of changes in energy absorption of specimens with 70, 80 and 90 percent openings area are depicted in Fig. 20 while Fig. 21 represents the diagram of changes in energy absorption of specimens with different forms for 70 to 90 percent openings area.

Generally speaking, with regard to energy absorption of the models shown in Figs. 20 and 21, the specimens in the second group have slight differences with each other and among them, the results of specimens with forms 1 and 3 and the results of specimens with forms 2 and 4 are almost identical. The amount of energy absorption change is about 2.5 to 3.5 percent for each 10 percent change in the area of the wall openings.

## 5. Conclusions

In the present study, a number of openings forms differing in terms of shape and location were defined in some steel shear wall specimens. The specimens divided into two groups: the first group included the specimens in which the openings area is less than half of the panel's area while the second group contained the specimens in which the area of the openings is more than half of the area of the panel. Six varied forms were assigned to the first group and four different forms to the second group. After verification of modelling process and analysis in the ABAQUS software through comparison of analytic results with experimental results of Vian's experimental model, each specimen was modelled and loaded up to 4.5 percent relative displacement and analyzed using nonlinear pushover analysis. The analyses' results were reported in some tables and compared in terms of stiffness, strength and energy absorption of specimens with the benefit of some carefully chosen diagrams. The conclusions of the present research can be summarized and listed as follows.

- Generally, it can be said that both shape and location of the openings affect the values of stiffness, strength and energy absorption.
- The curvier and with less sharp corners the openings are, the higher the values of stiffness and strength will be.
- The closer to the columns and further from the wall's center the openings are, the higher the stiffness and the strength will be. This was also observed by inspecting the stress contours of the imperforated shear wall. The parts of the wall's panel near the columns have borne the lowest stress. The highest stresses are seen in the diagonal direction of the parts of the wall's panel that are connected to the beams and in the central parts of the wall respectively. Therefore, for optimal use of the shear wall's panel it is suggested that the openings be preferably positioned in the wall according to the mentioned stress values.
- Having equal openings area percentage, the specimens with lower stiffness and strength are more responsive to increase in area of the openings and show more considerable changes in their seismic parameters.
- In some cases, for providing a required stiffness, the opening's shape and location can be chosen with regard to economic issues (opening area percentage and consumed steel material) and the type of opening's usage in the building service period.

## References

- Astaneh-Asl, A. (2001), "Seismic Behavior and Design of Steel Shear Walls", Steel TILS Report; Structural Steel Educational Council, July, Moraga, CA., USA.
- Astaneh-Asl, A. and Zhao, Q. (2002), "Cyclic Test of Steel Shear Walls-Final Report", Department of Civil and Environmental Engineering, College of Engineering, University of California at Berkeley, CA, USA.

- ATC Report 24 (1992), Guidelines for Seismic Testing of Components of Steel Structures; Applied Technology Council, Redwood City, CA, USA.
- Behbahanifard, M.R. (2003), "Cyclic Behavior of unstiffened Steel plate Shear Walls", Ph.D. Dissertation; Department of Civil Engineering, University of Alberta, Edmonton, Alberta, Canada.
- Berman, J. and Bruneau, M. (2003), "Plastic Analysis and Design of Steel Plate Shear Walls", *ASCE J. Struct. Eng.*, **129**, 11(1448).
- Bozdogan, K.B. (2013), "Free vibration analysis of asymmetric shear wall-frame buildings using modified finite element-transfer matrix method", *Struct. Eng. Mech., Int. J.*, **46**(1), 1-17.
- Darilmaz, K. (2017), "Dynamic behaviour of orthotropic elliptic paraboloid shells with openings", *Struct. Eng. Mech., Int. J.*, **63**(2), 225-235.
- Driver, R.G., Kulak, G.L., Laurie Kennedy, D.G. and Elwi, A.E. (1997), "Seismic behavior of steel plate shear wall", Structural Engineering Rep. No. 215; University of Alberta, Alberta, Canada.
- Driver, R.G., Kulak, G.L., Laurie Kennedy, D.G. and Elwi, A.E. (1998a), "Cyclic test of four-story steel plate shear wall", *ASCE J. Struct. Eng.*, **124**, 2(112).
- Driver, R.G., Kulak, G.L. and Kennedy, D.J.L. (1998b), "FE and simplified models of steel plate shear wall", *ASCE J. Struct. Eng.*, **124**, 2(121).
- Elgaaly, M., Caccese, V. and Du, C. (1993), "Post-buckling Behaviour of Steel-Plate Shear Walls Under Cyclic Loads", *ASCE J. Struct. Eng.*, **119**(2), 588-605.
- Farzampour, A., Laman, J.A. and Mofid, M. (2015), "Behavior prediction of corrugated steel plate shear walls with openings", *J. Constr. Steel Res.*, **114**, 258-268.
- Hibbit, Karlsson, & Sorenson, Inc. (HKS) (2003a), ABAQUS / Standard Theory Manual, Version 6.4, Hibbit, Karlsson, & Sorenson Inc., Pawtucket, RI, USA.
- Hibbit, Karlsson, & Sorenson, Inc. (HKS) (2003b), ABAQUS / Explicit User's Manual, Version 6.4, Hibbit, Karlsson, & Sorenson Inc., Pawtucket, RI, USA.
- Hosseinzadeh, S.A.A. and Tehranizadeh, M. (2012), "Introduction of stiffened large rectangular openings in steel plate shear walls", *J. Constr. Steel Res.*, **77**, 180-192.
- Kharrazi, M.H.K., Ventura, C.E., Prion, G.L. and Sabouri-Ghomi, S. (2004), "Bending and Shear Analysis and Design of Ductile Steel Plate Walls", *Proceedings of the 13<sup>th</sup> World Conference on Earthquake Engineering*, Vancouver, B.C., Canada, August.
- Kulak, G.L., Kennedy, D.J.L., Driver, R.G. and Medhekar, M. (2001), "Steel Plate Shear Walls: An Overview", *Am. Inst. Steel Constr. Eng. J.*, **38**, 50-62.
- Lubell, A.S. (1997), "Performance of unstiffened steel plate shear walls under cyclic quasi-static loading", M.Sc. Thesis; University of British Columbia, Vancouver, BC, Canada.
- Parulekar, Y.M., Reddy, G.R., Singh, R.K., Gopalkrishnan, N. and Ramarao, G.V. (2016), "Seismic performance evaluation of mid-rise shear walls: experiments and analysis", *Struct. Eng. Mech., Int. J.*, **59**(2), 291-312.
- Patil, A.N. and Dahake, A.G. (2014), "Design of steel plate shear wall with opening for steel building", *J. Struct. Eng. Manag.*, **1**(2), 17-24.
- Qu, B., Bruneau, M., Lin, C.H. and Tsai, K.C. (2008), "Testing of Full Scale Two-Story Steel Plate Shear Walls with RBS Connections and Composite Floors", *ASCE J. Struct. Eng.*, **134**, 3(364).
- Rezai, M. (1999), "Seismic behavior of steel plate shear walls by shake table testing", Ph.D. Dissertation; University of British Columbia, Vancouver, Canada.
- Sabelli, S.E.R. and Bruneau, M. (2006), "Steel Plate Shear Walls", AISC Design Guide 20.
- Schumacher, A., Grondin, G.Y. and Kulak, G.L. (1997), "Connection of infill Panels in Steel Plate Shear Walls", Structural Engineering Report No. 217; Department of Civil and Environmental Engineering, University of Alberta, Edmonton, Canada.
- Thorburn, L.J., Kulak, G.L. and Montgomery, C.J. (1983), "Analysis of Steel Plate Shear Walls", Structural Engineering Report No. 107; Department of Civil Engineering, University of Alberta, Edmonton, Canada.
- Timler, P.A. and Kulak, G.L. (1983), "Experimental study of steel plate shear walls", Structural Engineering Rep. No. 114; Department of Civil Engineering, University of Alberta, Alberta, Canada.
- Tromposch, E.W. and Kulak, G.L. (1987), "Cyclic and static behavior of thin panel steel plate shear walls", Structural Engineering Rep. No. 145; University of Alberta, Alberta, Canada.
- Valizadeh, H., Sheidaii, M. and Showkati, H. (2012), "Experimental investigation on cyclic behavior of perforated steel plate shear walls", *J. Constr. Steel Res.*, **70**, 308-316.
- Vian, D. and Bruneau, M. (2004), "Testing of Special LYS Steel Plate Shear Walls", *Proceeding of the 13<sup>th</sup> World Conference Earthquake Engineering*, Vancouver, Canada, Paper No. 978.
- Xue, M. and Lu, L.W. (1994), "Interaction of Infilled Steel Shear Wall Panels With Surrounding Frame Members", *Proceedings of Structural Stability Research Council Annual Technical Session*, Bethlehem, PA, USA, pp. 339-354.

CC